Simple new methods for deducing lifetimes in Recoil Distance Doppler-Shift measurements

P.Petkov[1] and C. Müller-Gatermann[2]
[1)]*STIINTA PENTRU TOTI S.R.L., Dionisie Lupu Str.33, Bucharest, Romania*
[2)]*Argonne National Laboratory, 9700 S. Cass Avenue Lemont, Il 60439, USA*

(*Electronic mail: pavel.p.petkov1956@gmail.com)

(Dated: 30 January 2022)

New approaches for lifetime determination using data from Recoil Distance Doppler-Shift experiments are presented based on fundamental properties of the functions describing the time evolution of the population of excited nuclear states. Partly, one of them represents a contraction of the well known Differential decay-curve method (DDCM) by using the most reliable data point (the maximum of the $n_i(t)$ function describing the population of level i in time) and purely numerical procedure avoiding any fitting of decay curves. The combination with the standard DDCM analysis is promising for improving the reliability and the precision of the results for the lifetimes obtained. The novel part of the approach consists of using a chain of equations at the consecutive maxima of the $n_i(t)$ functions which allow to precisely determine the ratio of the lifetimes of two consecutive levels and in the case where one of these lifetimes is known, to determine the unknown one. In addition, a simple integral derivation of the lifetime is presented involving the peak areas measured at different distances and an application of the first moments (expectation values, centroids in time) of the $n_i(t)$ functions for determining lifetime's is also demonstrated to be useful.

The Recoil-Distance Doppler-Shift (RDDS) or plunger method for lifetime measurements was originally based on recoil-into-vacuum of the residual nucleus after a nuclear reaction and the observation of γ-rays deexciting a particular investigated nuclear state at different target-to-stopper distances. During the flight, the γ-ray emission gives rise to a Doppler-shifted (S) peak as recorded by downstream or upstream detectors (i.e. sufficiently far from 90° about the direction of motion/flight). After coming at rest in a stopper, the depopulation of the excited state yields an unshifted (U) component in the detector spectrum. The relative intensities of these two components change when varying the target-to-stopper distance d (i.e. the flight-time $t_F = d/ < v >$ where $< v >$ is the mean recoil velocity). By investigating the evolution of the splitting of the total intensity into S- and U-components with d it is possible to determine the lifetime τ of the nuclear state studied. The feeding time from higher lying levels has to be also taken into account, indeed. More details about the basics of the plunger method can be found e.g. in the review articles[1–3].

Since about three decades, the differential decay-curve method (DDCM)[4,5] for the analysis of plunger data has proven to be very successful including the γ-γ coincidence case (as well as triples and more sophisticated coincidences, coincidences with particles etc.). Earlier approaches for analysis are discussed in detail in e.g. Refs.[1–3]. Independently of the data analysis approach, the precise determination of the areas of U and S peaks in the detector spectrum at each distance is of decisive importance for the reliability and precision of the derived lifetimes. Important problems arising during this determination were considered in details e.g. in Ref.[6] and solutions were proposed. These problems are: (i) poor separation of the U- and S-peaks due to a small Doppler-shift and/or wide velocity distribution of the recoils; (ii) modification of the line shape of the S-peak with the distance d; (iii) finite slowing-down time of the recoiling nuclei in the stopper which leads to Doppler-shift attenuation (DSA) of the energy of the emitted γ-rays giving rise to a continuous contribution to the spectrum. A review presenting thoroughly the developments along years, and especially in the last decades where the use of γ-γ coincidences became more and more efficient in solving the problem of the unknown (or side-) feeding, was done in Ref.[7].

With the present work, we would like to propose a new procedure for analyzing RDDS data. This procedure, while starting form the ideas of the DDCM, does not involve any fitting necessary for the lifetime determination and uses only data.

Let us remind the reader that the time evolution of a system of N nuclear levels is described (cf. e.g. Ref.[8]) by the solutions of a system of N differential equations:

$$\frac{dn_i(t)}{dt} = -\lambda_i n_i(t) + \sum_h \lambda_h b_{hi} n_h(t), \qquad (i = 1...N), \qquad (1)$$

where $n_i(t)$ describes the evolution of the population of the level of interest i, the levels h ($h > i$) are direct feeders of that level, $\lambda_{i,h}$ are the decay constants and b_{hi} are the branching ratios. The general solution (if $\lambda_k \neq \lambda_i$ for $i \neq k$) including all possible feeding levels (including not only the direct feeders, indeed) can be written in a straightforward way as shown in many textbooks and articles (c.f. again Ref.[8]).

$$n_i(t) = \sum_{k \geq i} C_{ik} e^{-\lambda_k t} = (n_i(0) - \sum_{k>i} C_{ik}) e^{-\lambda_i t} + \sum_{k>i} C_{ik} e^{-\lambda_k t}, \quad (2)$$

where $n_i(0)$ is the initial population (at $t = 0$) of the level i and the enumeration of the levels starts from it toward top. Recursive formulae are available in the literature which can be used to determine the coefficients C_{ik}. On the other hand, provided that the functions $n_h(t)$ of the direct feeders h are known, the solution of the set of equations 1 for every particular level i could be written as:

$$n_i(t) = n_i(0) e^{-\lambda_i t} + \sum_h \lambda_h b_{hi} \int_0^t dx n_h(x) e^{-\lambda_i (t-x)}. \qquad (3)$$

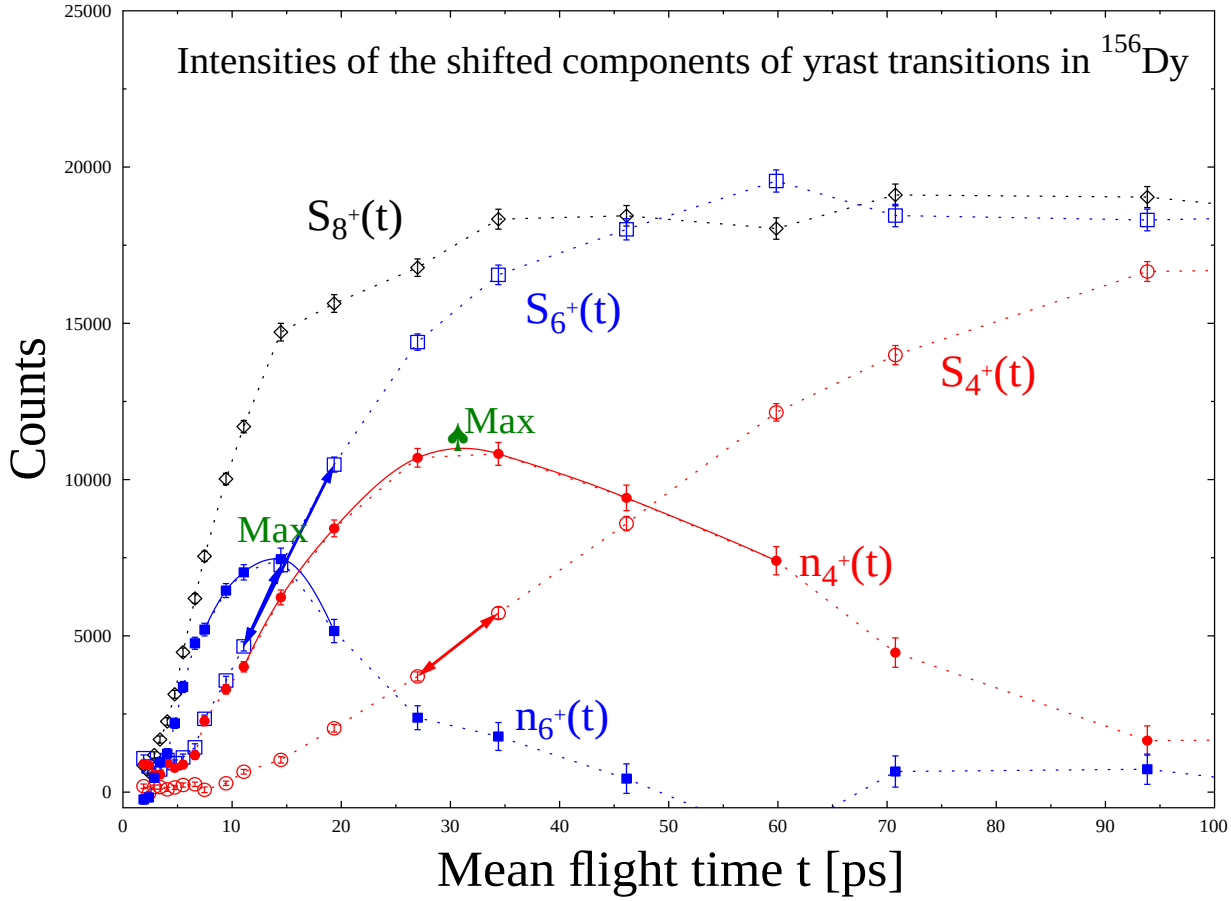

FIG. 1. Intensities $S(t)$ of the shifted components of the transitions depopulating the 8^+, 6^+ and 4^+ levels of belonging to the yrast band of ^{156}Dy as derived from the spectra gated on the U- and S-components of the $10^+ \rightarrow 8^+$ γ-ray transition as explained in the text. The intensities are presented with different symbols and their points are interconnected with dotted lines just for guiding the eye. The $n_i(t)$ functions of the 6^+ and 4^+ calculated using Eq.5 are also displayed. Some of their points around the maxima are interconnected with a smoothing function in order to facilitate the precise determination of the the position and heights of the maxima. Full lines with arrows on both ends indicated the intervals where the derivative $dS(t)/dt$ is calculated numerically. See also text and TableI.

Here, no details about the history of the population of the feeding levels h are present. However, this information is contained in the functions $n_h(t)$ themselves because they depend on the earlier stages of the cascade history. It should be mentioned that additional initial and logical (e.g. coincidence) conditions imposed could simplify the set of equations 1 and the function $n_i(t)$. The corresponding changes are easy to be introduced.

Below we will consider for simplicity a cascade of stretched γ-ray transitions as observed in the yrast bands of many even-even nuclei. Their absolute and even relative transition strengths are of primordial importance for nuclear structure investigations. In the following, an example of data and level scheme is taken from a previous study of ^{156}Dy[9]. Namely, the yrast band from the 8^+ level down is considered. By setting a gate on the full line-shape of the $10^+ \rightarrow 8^+$ transition (i.e. on both U- and S-components), all problems associated with side feeding (or unknown feeding) are eliminated. The chosen decay path in the even-even nucleus does not have the problem of contributions from transitions with different time-behavior, though known, feeding the levels of the yrast band from different non-yrast higher lying levels. Such contributions would appear in the case of a cleaning gate from below, e.g. on the $2^+ \rightarrow 0^+$ transition. At this situations, Eq.1 is reduced to

$$\frac{dn_i(t)}{dt} = -\lambda_i n_i(t) + \lambda_{i-1} n_{i-1}(t), \tag{4}$$

where all branchings b_{ij},b_{hi} are set to 1. It is easy to see that the condition for a maximum $dn_i(t)/dt$ =0 leads to the equation $\lambda_i n_i(t_i^{max})$=$\lambda_{i-1} n_{i-1}(t_i^{max})$ at the position of the maximum t_i^{max} of $n_i(t)$. In other words, the maximum of $\lambda_i n_i(t)$ lies on a point of the function $\lambda_{i-1} n_{i-1}(t)$ at t=t_i^{max} On the other hand, integrating Eq.4 from time zero to some time t yields:

$$\begin{aligned} n_i(t) &= \lambda_{i-1} \int_0^t n_{i-1}(t')dt' - \lambda_i \int_0^t n_i(t')dt' \\ &= S_{i-1}(t) - S_i(t). \end{aligned} \tag{5}$$

The integrals on the r.h.s. are proportional to the shifted decay curve $S(t)$ of the corresponding transition, which experimentally consists of the area of the shifted peak considered as function of the distance (flight time). Therefore, if one

measures experimentally the shifted decay functions $\tilde{S}_i(t)$ and $\tilde{S}_{i-1}(t)$, after corrections for detector efficiency, angular correlation/distribution effects and electron conversion of the γ-rays corresponding to the transitions populating and depopulating level i as well as taking into account higher order effects as change of the solid angle of detection with distance and possible deorientation of the nuclear spin, one can calculate $n_i(t)$ via Eq.5 as function of the flight time. Then, a very good estimate (one may call it even a "measure") of the position t_i^{max} and height of its maximum $n_i(t_i^{max})$ can be obtained. Obviously, the numerical estimate of the time-derivative of $S_i(t)$ at t_i^{max} yields immediately an estimate of the value of $\lambda_i n_i(t_i^{max})$ Dividing these quantities gives the lifetime of the level i

$$\tau_i = \frac{n_i(t_i^{max})}{\lambda_i n_i(t_i^{max})}. \tag{6}$$

This result can be directly obtained by using Eq. 9 below in the special case of b_{ij}=1 and one feeder (cf. also again Eq.5). As matter of fact, the value of τ_i derived in this way is simply a one-point sub-set (though the most reliable point) of the so-called $\tau(t)$-curve obtained in the framework of the DDCM analysis [4,5] because Eq. 6 is valid at any time t. In Ref.[4], the $\tau(t)$-curve is defined by Eq.13 in that work, namely

$$\tau_i = -\left[R_{ij}(t) - b_{ij}\sum_h R_{hi}(t)\right] / \left[dR_{ij}(t)/dt\right]. \tag{7}$$

Here, the unshifted components, denoted by R, of one depopulating transition ($i \rightarrow j$) and all directly feeding transitions $h \rightarrow i$ participate in the lifetime determination. Their sum is corrected by the branching ratio b_{ij} because if there is more than one depopulating transition the total feeding intensity splits among all of them, proportionally to the branching ratios. The intensities of the shifted and unshifted components are related to each other by the identities

$$R_{ij}(t) + S_{ij}(t) = R_{ij}(0) = S_{ij}(\infty) = const, \tag{8}$$

and therefore Eq.7 can be rewritten as

$$\tau_i = \left[b_{ij}\sum_h S_{hi}(t) - S_{ij}(t)\right] / \left[dS_{ij}(t)/dt\right]. \tag{9}$$

An advantage of the present approach is avoiding the fitting of $S_i(t)$ (with smoothly interconnected second order polynomials as a standard) over a wide time range and the use of only direct experimental quantities. Nevertheless, the parallel use of the $\tau(t)$-curve is extremely useful for checks for systematic errors and consistency, indeed. Such use will be presented in the practical example in ^{156}Dy below. It should be also mentioned that in the variant of the DDCM which is used most often in the coincidence regime (cf. e.g. Ref.[7]), gates from above on the shifted component (S) of the feeding transitions are applied because a gate on the unshifted component (U) in such case does not contain useful timing information.

Now, we turn our attention to one real novelty within the approaches that we would like to propose. Imagine a stretched cascade in an even-even nucleus with a gate set in γ-γ coincidence matrices on the transition depopulating the 10^+ level. All transitions below the $10^+ \rightarrow 8^+$ one, from the $8^+ \rightarrow 6^+$ to $2^+ \rightarrow 0^+$, have equal intensities and this is expressed in the γ-ray spectra by equal peak areas after corrections for the detection conditions (efficiency etc.). On the basis of Eq.4 and the comments following it, on may write the set (or chain) of equations

$$\begin{aligned} n_2(t_2^{max}) &= \frac{\lambda_4}{\lambda_2} n_4(t_2^{max}), \\ n_4(t_4^{max}) &= \frac{\lambda_6}{\lambda_4} n_6(t_4^{max}), \\ n_6(t_6^{max}) &= \frac{\lambda_8}{\lambda_6} n_8(t_6^{max}). \end{aligned} \tag{10}$$

The data on the l.h.s. can be easily deduced from the set of data points resulting from the subtraction of the experimental $S(t)$-curves of the γ-ray transitions belonging to consecutive pairs (cf. Eq.5). The next step is to adjust the factor f=λ_{i-1}/λ_i (we note that in Eqs.10 the lower indices are spins of levels, not level numbers within the standard convention) in order to scale the $n_{i-1}(t)$ function in such a way that the $n_i(t_i^{max})$ point lies on the former function after the scaling at the time point t_i^{max}. In a third step, the $\lambda_k n(t^{max})$ value for the lowest level k in the chain is obtained by simple numerical differentiation of the corresponding $S_k(t)$ function at the time point t^{max}. Then, Eq.6 can be applied to get τ_i and $\lambda_i = 1/\tau_i$. Knowing the adjusting factors f and λ_i for the lower level i, one can calculate λ_{i-1} for the feeding level, and repeat this step along the cascade for the higher lying levels each time obtaining a new λ (or τ) value for the feeding level in the pair. In a more general context, the chain of Eqs.10 allow a reliable measure of the ratio of the lifetimes (or of the decay constants) of every two consecutive transitions in the cascade.

Some other simple mathematical operations on the RDDS data my provide a quick estimate and even a reasonable value of the lifetime τ of the level of interest a. Let us consider the case of gate set on the shifted component of a γ-ray transition B populating directly that level a and originating from the decay of level b at time t_b. The gated transition A depopulating level a at time t_a splits into two components, unshifted (U), whose area depends on time (distance) as given by:

$$\begin{aligned} \{B_s, A_u\} &= \lambda_b \lambda_a \int_t^\infty dt'_a \int_0^t dt_b n_b(t_b) e^{-\lambda_a(t'_a - t_b)} \\ &= \lambda_b \int_0^t dt_b n_b(t_b) e^{-\lambda_a(t - t_b)} \\ &= n_a(t), \end{aligned} \tag{11}$$

and shifted (S):

$$\begin{aligned} \{B_s, A_s\} &= \lambda_b \lambda_a \int_0^t dt_a \int_0^{t_a} dt_b n_b(t_b) e^{-\lambda_a(t_a - t_b)} \\ &= \lambda_b \int_0^t dt_b n_b(t_b) - \lambda_b \int_0^t dt_b n_b(t_b) e^{-\lambda_a(t - t_b)} \\ &= S_b(t) - n_a(t) = S_a(t). \end{aligned} \tag{12}$$

The special notations in brackets indicate the gate on Doppler-shifted part of transition B_s (see subscript s) followed by transition A in two versions (A_s,A_u). Obviously, the integration

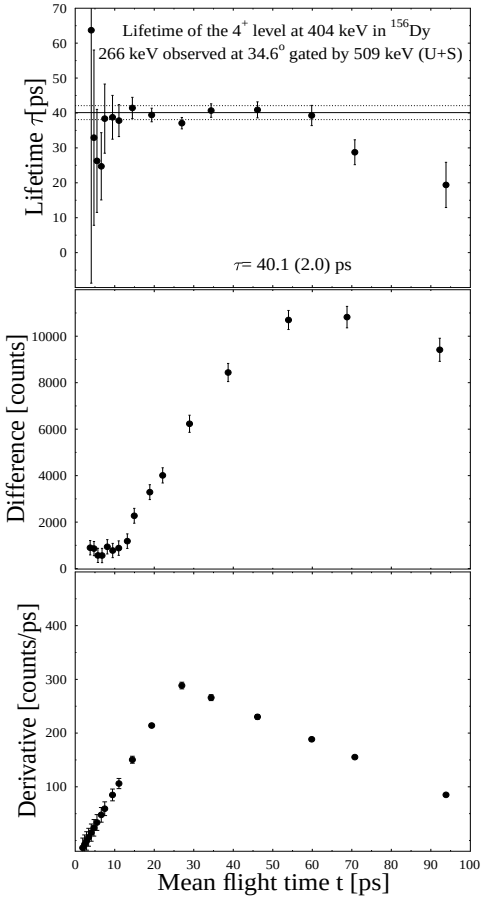

FIG. 2. Lifetime analysis at the 4_1^+ level. The panel in the middle shows the difference of the intensities of the shifted components of the $6^+ \rightarrow 4^+$ and $4^+ \rightarrow 2^+$ as derived from the spectra gated on the $10^+ \rightarrow 8^+$ and after normalization. The data in the bottom panel represent the time-derivative of the intensity of the shifted component of the $4^+ \rightarrow 2^+$ 266 keV transition obtained by a piecewise quadratic polynomial fit of that intensity. The panel on top illustrates the lifetime derivation according to the DDCM[4,5]. The value of the lifetime determined is also displayed. See also text and Eq.6.

over time from t=0 to $t \rightarrow \infty$ of the function $n_a(t)$ from Eq. 11 yields the intensity of the transition A divided by the decay constant λ_a, namely I_A^γ/λ_a. On the other hand, at $t \rightarrow \infty$, $n_a(t) \rightarrow 0$ and $S_b(\infty)$=$S_a(\infty)$. At such large times, there is not an unshifted component of the transition A and $S_a(\infty) = I_A^\gamma$ because the full intensity is a constant (experimentally, this may not be true for the measured shifted component due to effects of change of the observation solid angle, extranuclear effects as deorientation, see e.g. Ref.[1]). Therefore, one obtains in a simple way that

$$\tau_a = 1/\lambda_a = \frac{I_A^\gamma/\lambda_a}{I_A^\gamma} = \frac{\int_0^\infty n_a(t)dt}{S_a(\infty)}, \tag{13}$$

where the quantities in the numerator and denominator on the most r.h.s. are easily determined experimentally.

Another possibility for lifetime determination is given by the calculation of the expectation value $< n_a(t) >$ (or the first moment μ_1 over time) of the function $n_a(t)$. Using the definition for the expectation value of a non-normalized function in the interval t=0 to $t \rightarrow \infty$

$$\mu_1(f(t)) = \frac{\int_0^\infty f(t)tdt}{\int_0^\infty f(t)dt}, \tag{14}$$

and the results from Eqs.11,12, it is easy to show that

$$\mu_1 1(n_a(t)) = \mu_1(n_b(t)) + \tau_a. \tag{15}$$

The integral in the denominator of Eq. 14 is used for normalization. For the proof of Eq. 15 one has to consider the integrals needed for the calculation of the first moments:

$$\mu_1'(n_b(t)) = \int_0^\infty dt_b n_b(t_b) t_b, \tag{16}$$

and

$$\mu_1'(n_a(t)) = \lambda_b \int_0^\infty dt_a t_a \int_0^{t_a} dt_b n_b(t_b) e^{-\lambda_a(t_a - t_b)}, \tag{17}$$

where μ_1' indicates that these moments are non-normalized quantities. The order of integrations in Eq.17 can be inverted and the one over t_a performed first. The latter integration is taken as a partial one being similar to the general tabulated case of

$$\int dx x e^{-ax} = -\frac{1}{a} x e^{-ax} + \frac{1}{a} \int dx e^{-ax}. \tag{18}$$

The first term on the r.h.s. yields, for the case of Eq.17, the first moment of $n_b(t)$ while the second one yields a term proportional to τ_a. Thus, one obtains finally:

$$\mu_1 1'(n_a(t)) = \mu_1'(n_b(t)) + \tau_a I_a^\gamma \tag{19}$$

an analog of Eq.15, but for the non-normalized first moments. The quantity I_a^γ is the normalizing integral or the intensity of the transitions A (and B) in this simple case. Therefore, determining $\mu_1(n_a(t))$ by using the experimental data on $\{B_s, A_u\}$ as function of time (distance), and provided $\mu_1(n_b(t))$ is known, one may obtain a value for the lifetime τ_a of the level of interest. The information on $\mu_1(n_b(t))$ can be obtained by analyzing spectra generated by additional gates or by using numerical differentiation of $S_b(t)$ after its calculation by employing Eq.12.

Below, we present a practical application for the already mentioned case of one previous experiment[9]. Excited states in ^{156}Dy were populated using the reaction ^{124}Sn(^{36}S,4n) at a beam energy of 155 MeV. The beam was provided by the XTU Tandem of the Laboratori Nazionali di Legnaro, Italy. The target and stopper foils were mounted in the Cologne coincidence plunger[10] in which the change of the target-to-stopper distance is realized by moving the target holder. Additional details about the plunger set-up can be found in Ref.[10]. The target consisted of 0.9 mg/cm^2 Tin, enriched to 97.7% in ^{124}Sn, which was evaporated onto a 1.8 mg/cm^2 Ta foil serving as a backing facing the beam. A 12.0 mg/cm^2 Au foil was used to stop the recoils which were leaving the target with a mean velocity $< v >$ of 1.83(2)% of the velocity of light, c. The deexciting γ-rays were registered with the GASP array[11]

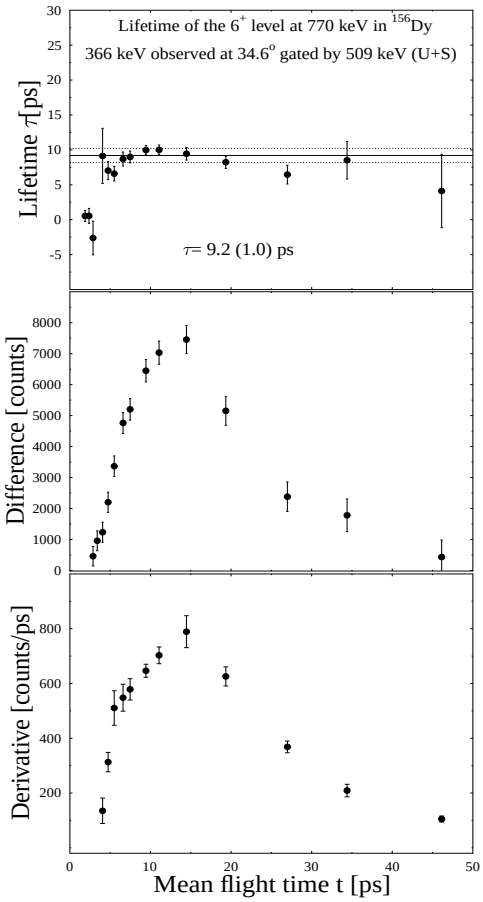

FIG. 3. The same as in Fig.2 but for the 6^+ level at 770 *keV*. See also text.

in its configuration I. For the data analysis, the 40 Germanium detectors were grouped into 7 rings (with approximately the same angle with respect to the beam axis). In the present work, we used the coincidence γ-γ matrices registering hits at ring 0 (mean angle with respect to the beam axis of 34.6°) and all 7 rings (i.e. coincidences between two detectors of ring 0 were also included). The 23 target-to-stopper distances where data were taken cover the range from 2.7 to 2902 μm. Normalization factors for the different distances were determined by using events corresponding to pairs of strong coincident transitions (cf. also Ref.[10]). More experimental details can be found in Ref.[9].

In the present work, gated spectra for the analysis of the RDDS data were obtained by setting a gate from above, on both U- and S- components of the transition of 509 *keV* depopulating the 10^+ level (see the level schemes in Refs.[9,12]. With this gate, the lifetimes of the 4^+ and 6^+ levels can be determined within the framework of the present approach. They are long enough to not require a treatment of the DSA effects (for emission during the deceleration in the stopper). The application of the new procedure is illustrated in Fig. 1. First, the areas of the S-peaks in the gated spectra were determined for the 445, 366 and 266 *keV* transitions depopulating the 8^+, 6^+ and 4^+ levels, respectively after a careful background subtraction. These areas ($S(t)$) are presented in Fig.1 with different open symbols after normalization. Correspondingly, the n_{4^+} and n_{6^+} functions (the populations of the levels as functions of the flight time t) were calculated according to Eq. 5 and also presented in Fig. 1. In Table I, the lifetime values derived in the present work by a simple and straightforward numerical analysis of the data in Fig. 1 are presented and compared to literature values. In addition, in Figs.2,3 a standard DDCM analysis is presented using the same data and employing the $\tau(t)$ curves displayed in the top panels to derive $\tau(4^+)$ and $\tau(6^+)$. Their values are also presented in Table I.

Concerning the use of Eqs.10 for lifetime derivation, on the basis of the data shown in Fig.1 and Table I, this can be easily done for the I^π=6^+ level. The maximum of the $n_{4^+}(t)$ function is positioned about t=30.7 *ps*. Dividing $n_{4^+}(t)$ by $n_{6^+}(t)$ leads to values of that ratio at the measured points of 27.0 and 34.4 *ps* of 4.49 (73) and 6.08 (1.5), respectively. A simple weighted average of these two values yields f=4.8(9) and an estimate of the lifetime of the 6^+ level of τ=8.6 (1.9). Thereby, the lifetime of the 4^+ as determined in the present work and given in column 8 of Table I was used. This result is in agreement with the value of $\tau(6^+)$ = 9.7 (1.1) *ps* from the present work and the value of 9.04 (15) *ps* from Ref.[9]. Similarly, by using the result for the 6^+ level in the 8^{th} column of Table I, one may calculate the lifetime of the 4^+ level as τ = 46.6 (8.0) ps via Eqs.10. Before the work of O. Möller et al.[9], lifetimes of the 6^+ level were quoted in the literature which are larger by 2 to 3 ps than the result of Ref.[9]. The latter result is nicely confirmed by the present work. It should be noted the points of the $n_{4^+}(t)$ function above 20 *ps* have large error bars and may be some systematic deviations originating mainly from the measured $S_{8^+}(t)$ shifted decay curve which displays some deviation from a smooth behavior (cf. Fig.1). We did not investigate in detail this problem since the aim of the present work is mainly a demonstration that the proposed procedures work than improving the precision of previously determined lifetimes. The latter might be possible, however, if data from all rings where significant Doppler-shifts are observed are averaged, and also by using a much larger number of gates on indirectly feeding transitions above the levels of interest. Yet the main purpose of the new procedures is providing reliable lifetime values in low-statistics cases and complement existing more precise methods for cross-checks.

In order to illustrate the last two new variants for lifetime determination (Eqs.13,14), spectra gated on the shifted component of the transition of 366 keV were used as seen by the detectors of ring 0 (mean angle with respect to the beam axis 34.6^o. The gates were set in the γ-γ coincidence matrices at the rings where sufficiently large Doppler-shifts are observed in the ^{156}Dy experiment considered. These are the rings with numbers 0,1,5,6 (see above, short description of the experiment and Ref.[9]). The corresponding spectra were analyzed and the normalized areas of the unshfted and shifted components of the 266 keV transition ($4^+ \rightarrow 2^+$) are displayed in Fig.4. The approach expressed by Eq.13 is indicated in the figure by the results for the time-integrated area of $n_{4^+}(t)$, which amounts to 710998 (6967) counts, and by the limiting value of $S_{4^+}(t \rightarrow \infty)$, i.e. at the largest distances measured, which is 16726 (386) counts. Dividing these two quantities

TABLE I. Lifetimes in ^{156}Dy derived in the present work. The energy of the level and its spin/parity are displayed in columns 1 and 2, respectively. The next column shows the energy of the depopulating stretched E2 γ-ray transitions. In the fourth and fifth columns, the position t^{max} of the maximum of the corresponding $n_i(t)$ function and the maximum value itself are displayed, respectively. The 6^{th} and 7^{th} columns show the quantities ΔS i.e. the difference of the S(t)-function values at the data points positioned the closest to the maximum at t^{max} and Δt, the time-difference between these points. These quantities are necessary for the numerical calculation of the derivative of $S(t)$ at t^{max} and are determined using the $S(t)$ functions in Fig.1. The next three columns present the lifetimes derived in the present work according to Eq.6, Eq.10 and using one of the standard procedures of the DDCM (cf. Figs.2,3). In the last column, lifetime values from Ref.[9] are shown for comparison. It should be mentioned that the latter values are derived using data with higher statistics generated by gates on direct feeders (and not somewhere above in the cascade as in the present work). The uncertainties of the experimental quantities are displayed in brackets. For presenting them, the convention of giving information on the last significant digits of the experimental quantities is used. In some cases, for this type of presentation digits before and after the decimal points is needed (e.g. 9.7 (1.1) means 9.7 $\pm$ 1.1) which is somewhat unconventional. Also unconventional is the presentation of the data on the counts (columns 5 and 6) which in principle should be rounded up. The only purpose for not doing this is the option left to reproduce the calculations in as much details as possible, if needed.

E^{lev} [keV]	I^{π}	E_{γ} [keV]	t^{max} [ps]	n(t^{max}) Counts	ΔS Counts	Δ t [ps]	τ (Eq.6) [ps]	τ (Eq.10) [ps]	τ_{DDCM} [ps]	τ_{lit} [ps]
404.2	4^+	266	30.1	11340(370)	2027(237)	7.4	41.4 (5.0)	46.6 (8.0)	40.1(2.0)	45.6(5)[9]
770.4	6^+	366	14.4	7454(354)	2600(260)	3.4	9.7 (1.1)	8.6 (1.9)	9.2(1.0)	9.04(15)[9]

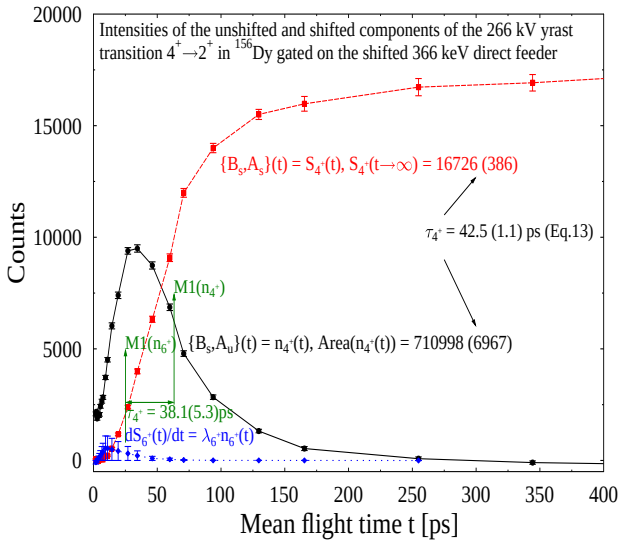

FIG. 4. Time (distance) dependence of the Intensities of the U- (filled circles) and S-components (filled squares) of the 266 keV γ-ray transition depopulating the 4^+ level belonging to the yrast band of ^{156}Dy and gated on the shifted component of the directly feeding $6^+ \rightarrow 4^+$ transition. The data points are interconnected by lines just for guiding the eye. The first moment $M1(n_{6^+})(t))$ is calculated using numerical differentiation of $S_{6^+}(t)$. The latter time-derivative is displayed with filled diamonds and is characterized by relatively large error bars. This explains the somewhat large uncertainty of the 4^+ lifetime (38.1(5.3) ps) as calculated using the difference of the first moments (Eq.14). The lifetime of the 4^+ level calculated using Eq.13 is also indicated. See also text.

leads to the result $\tau(4^+) = 42.5$ (1.1) ps. Preliminary applications of this approach in a slightly different version[13] indicate that it is very useful in the case where it is necessary to estimate a given lifetime on the basis of low statistics data. Thus, in Ref.[13] neutron-rich even-even Se nuclei were produced via neutron-transfer reactions using a ^{82}Se beam, and the yield for the most neutron-rich ones (A$\geq$84) was very low. Concerning the use first moments M1 (Eq.14), the subtraction leads, as also indicated in Fig.4, to the result of $\tau(4^+) = 38.1$ (5.3) ps. Both values are in good agreement with the results displayed in the first row of Table I, including the literature value from Ref.[9].

The new approaches using features of the solutions of the Bateman equations, which was presented in the context of the RDDS method, may find application in the framework of other methods for lifetime determination. Namely, this is valid for measurements where the functions $n_i(t)$ describing the behavior of the population of the level i in time can be measured (or, more often, the functions $\lambda_i n_i(t)$) with enough precision. In principle the so-called Electronic timing[14,15], also in its modern version, the Fast timing (cf. e.g. Refs.[16,17]), is very suitable for this purpose. The difficulty here is that the measured data (or time distributions) are detected physically as a convolution of $\lambda_i n_i(t)$ with the detector response function $P(t)$ (or prompt time distribution) due to the finite time resolution of the detecting system:

$$D_{ij}(t) = b_{ij} \int_{-\infty}^{t} P(y)\lambda_i n_i(t-y)dy. \qquad (20)$$

Since the shape of the prompt time distribution is dependent on the γ-ray energy in a more or less complicated way, a direct use of the new approach is not possible. This problem can be circumvented by means of deconvolution of the measured time distributions leading to determination of $\lambda_i n_i(t)$ with some precision, in most of the cases probably inferior to that obtained in the RDDS case.

Another method for lifetime determination, where finding out the decay function $\lambda_i n_i(t)$ is again analog to solving an integral equation (as is Eq.20) is the Doppler-shift attenuation method (DSAM) (see e.g. Ref.[1,3] for comprehensive reviews). There are many variants for analyzing the data, especially in γ-γ coincidences. In the most simple case of singles DSAM measurements, the detected line shape $S_\theta(E)$ at a given observation angle θ (e.g. with respect to the direction of motion of the nucleus decelerating in a given material medium)

is obtained by folding the spectrum of Doppler-shifted energies E_θ^{Sh} with the detector response function $\Phi(E, E_\theta^{Sh})$. It is commonly described by the following formula

$$S_\theta(E) = b_{ij} \int_{-\infty}^{\infty} dE_\theta^{Sh} \Phi(E, E_\theta^{Sh}) \int_0^{\infty} dt P_\theta(t, v_\theta) \lambda_i n_i(t). \quad (21)$$

The quantity $P_\theta(t, v_\theta)$ is the stopping matrix which represents the normalized distributions of the velocity projection v_θ on the observation axis at different times t and is calculated using Monte Carlo simulations (cf. Ref.[18]). The stopping matrix plays the role of the kernel of the integral equation given by Eq.21. Again the precision of the determination of $\lambda_i n_i(t)$ in most of the cases is probably inferior to that obtained in the RDDS case, yet it offers a possibility to apply the new approaches from the present work.

To conclude, new approaches for lifetime determination using data from RDDS (plunger) experiments were presented. Fundamental properties of the functions describing the time evolution of the population of excited nuclear states are used to derive the lifetime τ of a given level. One of the versions represents simply a contraction of the well established Differential decay-curve method (DDCM) by using the most reliable data point (the maximum of the function $n_i(t)$ describing the population in time) and purely numerical procedure avoiding any fitting except this of the γ-ray spectra. The combination with the standard DDCM analysis is promising for improving the reliability and the precision of the results for the lifetimes obtained. The second, really novel part of the approach consists of using a chain of equations at the consecutive maxima of the $n_i(t)$ functions which allow to precisely determine the ratio of the lifetimes of two consecutive levels and in the case where one of these lifetimes is known, to determine the unknown one. Further, a simple integral derivation of the lifetime was presented based on peak areas and of use in cases of RDDS data with very low statistics. Finally, using differences of the first moments (expectation values, centroids in time) of the $n_i(t)$ functions yields also useful results. Although biased by mathematical difficulties, this chain of equations may be used in other methods for lifetime determination apart fromm the RDDS.

Acknowledgments: The authors are indebted to Dr. I. Penev for valuable comments and discussions.

Data Availability:

The data analyzed and used to illustrate the findings of this methodological study are available from the corresponding author upon request.

[1] T. K. Alexander and J. S. Forster, in *Advances in Nuclear Physics* v.10, p.197, Eds. M. Baranger and E. Vogt, Plenum Press, 1978
[2] P. J. Nolan and J. F. Sharpey-Schafer, Rep. Prog. Phys. 42, 1 (1979).
[3] K.P.Lieb, in *Experimental Techniques in Nuclear Physics*, Eds. D. N. Poenaru and W. Greiner, (Walter de Gruyter, Berlin-New York 1997), p.425
[4] A. Dewald, S. Harissopulos and P. von Brentano, Z. Phys. A 334 163 (1989).
[5] G. Böhm, A. Dewald, P. Petkov and P. von Brentano, Nucl. Instr. Meth. Phys. Res. A 329, 248 (1993).
[6] P. Petkov, D. Tonev, J. Gableske, A. Dewald, T. Klemme and P. von Brentano, Nucl. Instr. Meth. Phys. Res. A 431, 208 (1999).
[7] A. Dewald, O. Möller and P. Petkov, Prog. Part. Nucl. Phys. 67, 786 (2012).
[8] E. Segre, in Nuclei and Particles, W.A.Benjamin, Inc., New York 1965, p.157
[9] O. Möller, A. Dewald, P. Petkov, B. Saha, A. Fitzler, K. Jessen, D. Tonev, T. Klug, S. Heinze, J. Jolie, P.von Brentano, D. Bazzacco, C. A. Ur, E. Farnea, M. Axiotis, S. Lunardi, G. de Angelis, D. R. Napoli, N. Marginean, T. Martinez, M. A. Caprio and R. F. Casten, Phys. Rev. C74, 024313 (2006).
[10] A. Dewald, P. Sala, R. Wrzal, G. Böhm, D. Lieberz, G. Siems, R. Wirowski, K. O. Zell, A. Gelberg, P. von Brentano, P. Nolan, A. J. Kirwan, P. J. Bishop, R. Julin, A. Lampinen and J. Hattula, Nucl. Phys. A 545, 822 (1992).
[11] D. Bazzacco, in *Proc. Int. Conf. on Nuclear Structure at High Angular Momentum*, Ottawa, 1992, Chalk River Report (AECL 10613), p.386
[12] C. W. Reich, Nuclear Data Sheets 113, 2537 (2012).
[13] J. Litzinger, Dissertation, University of Cologne, 2018.
[14] Z. Bay, Phys. Rev. 77, 419 (1950).
[15] K. E. G. Löbner, in *The Electromagnetic Interaction in Nuclear Spectroscopy*, Ed. W. D. Hamilton, (North-Holland, New York, 1975), p. 173.
[16] H. Mach, R. L. Gill, and M. Moszynski, Nucl. Instr. Meth. Phys. Res. A 280, 49 (1989).
[17] J.-M. Régis et al., Nucl. Instr. Meth. Phys. Res. A 726, 191 (2013).
[18] W. M. Currie, Nucl. Instr. Meth. 73, 173 (1969).